ELSEVIER

Journal of Organometallic Chemistry 628 (2001) 114–122

Journal of Organometallic Chemistry

www.elsevier.nl/locate/jorganchem

Chiral aminophosphonite-phosphite ligands: synthesis and use in platinum- and rhodium-based enantioselective hydroformylation of styrene. Crystal structure of [(*S*)-*N*-(2,2′biphenoxyphosphino)-2-(2,2′biphenoxyphosphinoxymethyl)pyrrolidine]-dichloroplatinum(II)

Said Naili [a], Isabelle Suisse [a], André Mortreux [a], Francine Agbossou-Niedercorn [a,*], Guy Nowogrocki [b]

[a] *Laboratoire de Catalyse de Lille, Groupe de Chimie Organique Appliquée, ESA 8010, Ecole Nationale Supérieure de Chimie de Lille, B.P. 108-59652 Villeneuve d'Ascq Cedex, France*

[b] *Laboratoire de Cristallochimie et de Physicochimie du Solide, ESA 8012, Ecole Nationale Supérieure de Chimie de Lille, B.P. 108-59652 Villeneuve d'Ascq Cedex, France*

Received 5 January 2001; accepted 5 March 2001

Abstract

New chiral unsymmetrical ligands containing deficient phosphorous moieties based on (*S*)-prolinol and (*S*)-oxoprolinol have been synthesised and used as chiral auxiliaries for the platinum- and rhodium-catalysed enantioselective hydroformylations of styrene. The new ligands are obtained readily by reaction of the amino alcohols with a chlorophosphonite. The beneficial effect induced by the electron-deficient phosphorous ends provided the branched aldehyde in up to 44% ee. A crystal structure of the platinum complex **5** is described. © 2001 Elsevier Science B.V. All rights reserved.

Keywords: Platinum; Rhodium; Hydroformylation; Diphosphine; Phosphonite–phosphite

1. Introduction

Asymmetric hydroformylation of olefins is a very attractive process for the synthesis of optically pure aldehydes. The latter are useful as building blocks for the preparation of pharmaceuticals, agrochemicals and food additives [1]. The 2-arylpropionic acids, readily obtained by oxidation of the corresponding chiral aldehydes, which constitute aclass of nonsteroidal anti-inflammatory drugs with substantial pharmaceutical and commercial impact [2] are very good examples. Platinum and rhodium complexes modified by chiral phosphanes have been the most-employed hydroformylation catalysts [3]. Importantly, the recent development of rhodium-based asymmetric hydroformylation involving chiral bidendate phosphine–phosphites [4] or diphosphites [5] allowed access to highly *regio* and *enantioselective* processes. However, until the breakthrough of Takaya and co-workers with the phosphine–phosphite-Rh(I) catalysts [4a], the diphosphane-platinum(II) catalysts promoted by $SnCl_2$ were the most popular as they led to the highest enantioselectivities [3,6] even if their utilisation is often accompanied by low regioselectivities to the branched aldehydes and low reaction rates.

We and others [7] have already reported on the synthesis, characterisation, and use of aminophosphine–phosphinites (AMPP) in Rh- and Pt-catalysed styrene hydroformylations. The interest of such ligands lies in their unsymmetrical nature, which offers distinct advantages from those of the symmetrical auxiliaries. Considering the specific ability presented by the bisphosphite-based catalytic systems mentioned above, we sought to synthesise new ligands derived from amino

* Corresponding author. Tel.: +33-3-20434927; fax: +33-3-20436585.

E-mail address: agbossou@ensc-lille.fr (F. Agbossou-Niedercorn).

PII: S0022-328X(01)00768-9

alcohols, including such electron-deficient — yet achiral — phosphorous moieties. Actually, chiral symmetrical diphosphite–platinum catalysts have been reported recently providing as high as 91% ee in the hydroformylaton of styrene [6e]. Here, we wish to present our results on the synthesis of two new homochiral aminophosphonite–phosphite chelates possessing bisphenol moieties on the two phosphorous atoms and on their use in enantioselective hydroformylation of the model substrate styrene. We also describe an X-ray structure of a platinum complex chelated by one of these new ligands.

2. Results and discussion

2.1. Synthesis and characterisation of the ligands and platinum complexes

From our studies on the AMPP ligands, two chiral precursors have appeared to be particularly suited for their potential as chiral auxiliaries for enantioselective processes, i.e. (*S*)-2-(hydroxymethyl)pyrrolidine (**1**) and (*S*)-2-(hydroxymethyl)pyrrolidinone (**2**) (Scheme 1) [8]. Consequently, the latter have been selected for investigation in the synthesis of new ligands for asymmetric hydroformylation. The synthesis of the new ligands paralleled the route developed for the access to AMPPs. First, (*S*)-2-(hydroxymethyl)pyrrolidine (**1**) was reacted with 2,2′-bisphenoxyphosphorous chloride (BPPCl) [9] in the presence of triethylamine in tetrahydrofuran (THF) at 60°C (Scheme 1).

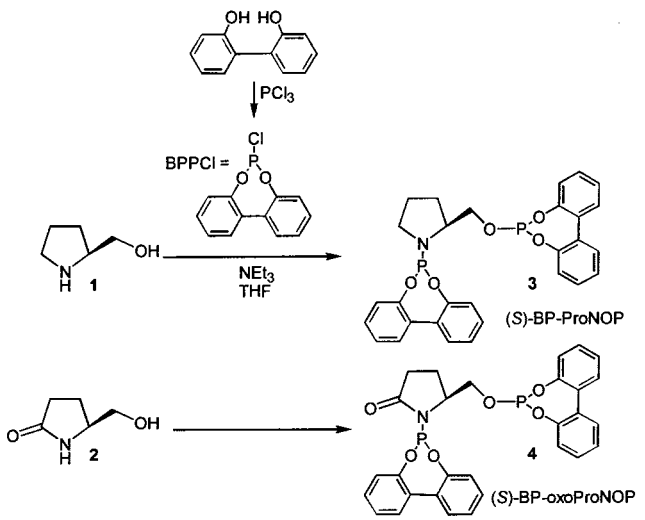

Scheme 1.

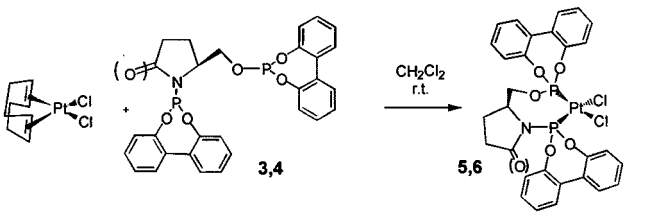

Scheme 2.

The ligand formation was monitored by ^{31}P-NMR spectroscopy. Indeed, the signal of the starting chloride at 178 ppm decreased in favour of the ligand signals. Thus, after 18 h stirring at 60°C, two major peaks remained at 150 and 138.7 ppm attributed to the P(O) and P(N) phosphorous atoms of (*S*)-BP-ProNOP (**3**). Then, the triethylamine hydrochloride formed was separated under nitrogen via a simple filtration through basic alumina providing ligand **3** after solvent removal as a white powder in 88% yield. Ligand **3** afforded satisfactory elemental analysis and was characterised by NMR spectroscopy. Data are summarised in Section 4. Since we suspected an inversion of the relative position of the two ^{31}P-NMR signals [10],[1] we carried out a 2D ^{31}P, ^{1}H experiment. Generally, in agreement with the relative electronegativities of the O and N atoms, in the ^{31}P-NMR spectra, the P(O) signal is downfield from that of the P(N) one. The 2D ^{31}P-, ^{1}H-NMR cross-peaks obtained with both phosphorous atoms and the protons of the chiral skeleton corroborate our assignment of the ^{31}P-NMR signals. Indeed, cross-peaks are obtained between the P(O) resonance at 150 ppm and the protons of the N–CH^1–CH^2H^3O chain (δ 3.85 (H^1), 3.85 (H^2), and 3.67 (H^3)) and the protons of the bisphenoxy moiety (δ 6.95–7.39), whereas the P(N) at 138.7 ppm correlates with the protons on the carbon atoms adjacent to the nitrogen atom CH_2NCH at δ 3.85 and with the aryl protons of the bisphenoxy residue. In addition, a coupling is observed between both phosphorous atoms and the stereogenic carbon atom as the signal of the latter appears as a doublet of doublets ($J_{CP} = 25$ and 3 Hz) in the ^{13}C{^{1}H}-NMR spectrum of **3**.

In a similar manner, the precursor (*S*)-2-(hydroxymethyl)pyrrolidinone (**2**) has been reacted with BPPCl in order to provide (*S*)-BP-oxoProNOP (**4**) (Scheme 1). The workup was carried out as above, furnishing **4** as a white powder in 86% yield. Derivative **4** presents ^{31}P-NMR signals as singlets at 145 (P(O)) and 137 ppm (P(N)). However, ligand **4** is less stable than **3** and only a small pad of alumina could be used for the filtration used for the purification. Indeed, the P–N bond is more fragile in **4** than in **3** and the monosubstituted aminophosphite derivative HN–OP is produced easily. This substantial fragility did not allow the isolation of an analytically pure **4**. Nevertheless, the purity was high enough (> 95% by ^{31}P-NMR) for an evaluation in catalysis.

[1] Such a trend has been observed for ephedrine-based aminophosphonite–phosphite ligands

Table 1
Crystal data and structure refinement parameters for [$PtCl_2$\{(*S*)-BP-ProNOP\}] (**5**·CH_2Cl_2)

Empirical formula	$C_{29}H_{25}Cl_2NO_5P_2Pt{\cdot}CH_2Cl_2$
Formula weight	880.3866
Temperature (K)	295
Colour and habit	Colourless prism
Crystal system	Orthorhombic
Space group	$P2_12_12_1$ (SG: 19)
Unit cell dimensions	
a (Å)	12.822(4)
b (Å)	13.364(2)
c (Å)	18.382(3)
V (Å^3)	3150
θ range for acc. cell (°)	10
Z	4
D_{calc} (g cm^{-3})	1.674
F(000)	1720
Crystal size (mm)	$0.30 \times 0.20 \times 0.20$
μ(Mo–K_α) (cm^{-1})	49.9
θ range for data collection (°)	2–28
Scan type	$\omega/2\theta$
Crystal description	Irregular, ovoid
Number of data collected	8184
Number of unique data	7241
hkl Ranges	0.16, 0.17, −23.23
R_{merge}	0.044
Standard reflections	($\underline{4}10$); ($\underline{1}31$); ($\underline{4}10$)
Observability criterion, *n* [$I > n\sigma(I)$]	3
Number of data in refinement	5571
Number of refined parameters	407
Final *R*	0.0390
R_w	0.045
Largest difference peak and hole (e Å^{-3})	2.1 and −1.5

Next, the platinum catalytic precursors Pt{(*S*)-BP-ProNOP}Cl_2 (**5**) and Pt{(*S*)-BP-oxoProNOP}Cl_2 (**6**) were synthesised in dichloromethane at room temperature by reacting Pt(COD)Cl_2 with an equimolar amount of ligands **3** and **4**, respectively (Scheme 2).

The synthesis of **5** proceeded very readily at room temperature and was almost quantitative, providing, after workup, an off-white air-stable solid. The characterisation of **5** was carried out through elemental analysis, NMR spectroscopy and X-ray crystallographic analysis. Data are summarised below and in Section 4. The ^{31}P-NMR signal trend established a chelation of ligand **3** to the platinum centre. In fact, the P(O) and P(N) resonances consist of two sets of doublets of similar intensity at 85 and 72 ppm. These main signals are supplemented with the two doublets of doublets constituting the ^{195}Pt satellites. The large values of the $^1J_{(Pt-P)}$, i.e. 5392 Hz for $^1J_{(Pt,P(O))}$ and 5792 Hz for $^1J_{(Pt,P(N))}$ associated to the small $^2J_{(P,P)}$ value (28 Hz) are consistent with a *cis* geometry [11,12]. In addition, the Pt–P coupling constants are greater than those observed for the AMPP analogues by an average of 1500 Hz of magnitude. It is well known that for a given type of metal complex, when changing from a phosphine to a phosphite ligand, a variation in $^1J_{(M,P)}$ of between 50 and 100% is observed [11,12]. For complex **5** (and **6** below) it is thus not surprising to observe also a significant increase of $^1J_{(Pt-P)}$. In addition, a parallel shortening of the Pt–P bonds is foreseen and was, indeed, observed (see the X-ray characterisation below). Ordinarily, a deshielding is observed for both the P(O) and P(N) phosphorous atoms upon coordination of AMPP ligands to rhodium [8b], palladium [13] or ruthenium [14]. In the case of platinum complexes, commonly, the P(O) signal is upfield from that of the free ligands and the P(N) slightly downfield [7c,d]. It is noteworthy to mention that, here, both phosphorous resonances of the ligand in complex **5** appear ca. 60 ppm upfield from that of the free ligand. These shieldings are in the range usually observed for phosphite-type complexes when compared to the phosphine-based platinum species [15].

The reaction of Pt(COD)Cl_2 with **4** provided Pt{(*S*)-BP-oxoProNOP}Cl_2 (**6**) quantitatively. The latter exhibits ^{31}P-NMR signals as two doublets at 90 and 86 ppm ($^2J_{(P,P)} = 4.2$ Hz) accompanied by the ^{195}Pt satellites, the $^1J_{(Pt,P(O))}$ and $^1J_{(Pt,P(N))}$ being 5658 and 5833 Hz, respectively. Both complexes **5** and **6** are stable in air in the solid state and in solution.

2.2. Crystal structure of **5**

Slow crystallisation from dichloromethane of the crude complex **5** afforded colourless crystals, which proved suitable for an X-ray investigation. X-ray data were collected under the conditions summarised in Table 1 and atomic coordinates are given in Table 2. Refinement described in Section 4 gave the structure shown in Fig. 1 together with the numbering scheme adopted, and showed the product to be a CH_2Cl_2 monosolvate monomeric complex. Selected key bond lengths, bond angles, and deviations from the mean plane Pt–Cl–Cl–P(O)–P(N) are listed in Table 3.

The *cis* geometry was established by the X-ray data. As evidenced from the deviations from the mean plane Pt–Cl–Cl–P(O)–P(N), complex **5**·CH_2Cl_2 adopts a conformation around Pt close to that of an idealised square planar geometry (average deviation 0.010(2) Å). Complex **5**·CH_2Cl_2 exhibits Pt–P(O) and Pt–P(N) lengths (2.190(3) and 2.202(2) Å) distinctly shorter than those in other structurally characterised AMPP complexes by an average of 0.027 and 0.029 Å, respectively [7c,d,16,17]. These two characteristics, as mentioned above, are a consequence of the substitution of the phosphorous atoms by the electronegative bisphenoxy moiety. Complex **5**·CH_2Cl_2 exhibits equal Pt–Cl bond lengths (2.331 Å) and similar Cl–Pt–P angles (89.76 (11) and 91.51(11)°), indicating that the two BP adducts induce the same steric hindrance around platinum.

There is only a very small widening of the bite angle P(O)–Pt–P(N) (91.66(11)°). The latter is overall smaller than those in other AMPP–Pt complexes [16]. Other geometric features were calculated. For example, the out-of-plane distortion between the aryl rings in both bisphenol units has been quantified. Thus, the angle between the planes defined by the adjacent least-square planes defined by the aryl carbons of the BP units are 38.7 and 38°, respectively, on the P(N) and P(O) sides of the complex, showing thus a small distortion from initial bisphenol planarity. The deviations of the aryl carbon atoms from the corresponding planes were less than 0.019 Å. The sum of the angles around nitrogen is 359.98°, which shows that the nitrogen atom has an sp^2 hybridisation. The sums of the bond angles around both P(N) and P(O) phosphorous atoms are 307.61 and 313.31°, respectively. These values indicate conformations intermediate between pyramidal and tetrahedral. Seven-membered rings can adopt several boat and chair conformations. Hence, some of them have already been noticed for AMPP and related complexes, which is indicative of the overall flexibility of the AMPP ligands [16,17]. That flexibility potential proves that the AMPP moieties can accommodate the steric requirement of the metal and of the other ligands present in the coordination sphere. Complex **5**·CH_2Cl_2 exhibits an almost pure twist boat conformation with the oxygen atom of the P(O) unit very close to the plane defined by Pt–Cl–Cl–P(O)–P(N) (deviation 0.234(6) Å) (Fig. 2). The nitrogen atom of the P(N) residue deviates 1.286(6) Å from that plane. Such a metallacycle conformation is generally observed in (*S*)-Ph,Ph-ProNOP complexes [7c,14].

Table 2
Atomic coordinates and equivalent isotropic displacement parameters for [$PtCl_2$\{(*S*)-BP-ProNOP\}] (**5**·CH_2Cl_2)

Atom	*x*/*a*	*y*/*b*	*z*/*c*	B_{eq} (Å^2)
Pt(1)	0.03082(2)	0.00225(3)	0.09258(1)	2.66(1)
Cl(2)	0.0044(2)	−0.1349(2)	0.1687(1)	4.81(7)
Cl(3)	0.1788(2)	−0.0802(2)	0.0499(1)	4.25(6)
P(4)	0.0595(2)	0.1302(2)	0.0198(1)	2.44(4)
P(5)	−0.1114(2)	0.0714(2)	0.1352(1)	2.80(5)
O(6)	−0.1349(5)	0.1841(4)	0.1156(3)	3.3(1)
C(7)	−0.0752(8)	0.2682(6)	0.1419(5)	3.7(2)
C(8)	0.0423(7)	0.2549(6)	0.1371(4)	3.3(2)
N(9)	0.0756(5)	0.2366(5)	0.0605(3)	2.8(2)
C(10)	0.1211(8)	0.3295(6)	0.0296(5)	3.6(2)
C(11)	0.1744(8)	0.3769(7)	0.0956(5)	4.4(3)
C(12)	0.0958(9)	0.3547(7)	0.01574(5)	4.6(3)
O(13)	−0.2204(5)	0.0289(4)	0.1082(3)	3.2(1)
O(14)	−0.1159(4)	0.0619(4)	0.2219(3)	3.2(1)
O(15)	0.1609(4)	0.1292(4)	−0.0304(3)	2.9(1)
O(16)	−0.0321(4)	0.1357(4)	−0.0391(3)	2.8(1)
C(17)	0.1678(7)	0.1044(6)	−0.1049(4)	3.1(2)
C(18)	0.2423(8)	0.0324(7)	−0.1197(5)	4.2(2)
C(19)	0.2640(9)	0.0174(8)	−0.1962(6)	5.0(3)
C(20)	0.2130(10)	0.0729(9)	0.2483(65)	5.7(3)
C(21)	0.1361(8)	0.1419(8)	−0.2291(5)	4.4(3)
C(22)	0.1127(7)	0.1611(6)	−0.1568(4)	3.3(2)
C(23)	0.0337(7)	0.2361(6)	−0.1369(4)	3.3(2)
C(24)	0.0287(9)	0.3245(7)	−0.1772(5)	4.7(3)
C(25)	−0.0472(10)	0.3966(9)	−0.1611(7)	6.1(4)
C(26)	−0.1186(9)	0.3823(8)	−0.1052(6)	5.6(3)
C(27)	−0.1124(8)	0.2928(7)	−0.0653(5)	4.2(3)
C(28)	−0.0369(7)	0.2232(6)	−0.0821(4)	3.0(2)
C(29)	−0.2519(7)	−0.0694(7)	0.1331(5)	3.7(2)
C(30)	−0.2505(8)	−0.1440(8)	0.0798(5)	4.6(3)
C(31)	−0.2851(10)	−0.2371(8)	0.1008(7)	5.9(4)
C(32)	−0.3220(9)	−0.2528(8)	0.1721(7)	5.6(3)
C(33)	−0.3231(8)	−0.1743(6)	0.2222(6)	4.1(2)
C(34)	−0.2863(7)	−0.0796(6)	0.2025(4)	3.1(2)
C(35)	−0.2865(6)	0.0017(8)	0.2565(4)	3.3(2)
C(36)	−0.3714(6)	0.0093(9)	0.3064(4)	3.8(2)
C(37)	−0.3715(8)	0.0869(8)	0.3578(5)	4.2(3)
C(38)	−0.2910(9)	0.1579(8)	0.3600(5)	4.2(3)
C(39)	−0.2086(8)	0.1510(7)	0.3120(4)	3.7(2)
C(40)	−0.2070(6)	0.0721(6)	0.2623(4)	2.8(2)
C(41)	0.002(1)	0.686(1)	0.032(1)	10.5(7)
Cl(42)	−0.053(1)	0.672(2)	−0.043(1)	13.7(8)
Cl(43)	−0.008(2)	0.582(2)	0.077(1)	14.2(8)

2.3. Catalysis

The two ligands **3** and **4** have been evaluated in the platinum- and rhodium-based hydroformylations of styrene (Table 4). The platinum catalysts were obtained from the reaction of complexes **5** and **6** with one equivalent of $SnCl_2·2H_2O$ as a promoter. Rhodium catalysts were prepared by mixing $Rh_4(CO)_{12}$ in toluene with ligands **3** and **4** (Rh–ligand = 1.5). The hydroformylation reactions were carried out under classical reaction conditions (Table 4) and provided a mixture of the branched (*b*) (2-phenylpropanal) and the linear (3-phenylpropanal) (*n*) regioisomers along with the hydrogenated side-compound for platinum-based catalyses (Scheme 3).

For platinum-based reactions, the activity of the catalytic system obtained in this study was in the average observed for platinum catalysts [3]. Nevertheless, compared to our own previously reported AMPP–Pt catalysts [7c], a beneficial effect on both the activity and the regioselectivity was achieved. The latter could be ascribed to the bisphenoxy moiety. For instance, the mixture of branched and linear aldehydes was produced in a *b*/*n* ratio ranging from 53/47 to 66/34, whereas earlier ligands provided only ratios in the 30/70–43/57 range [7c]. In addition, turnover frequencies varying from 15 to 38 h^{-1} were measured here. These values have to be compared to those acquired with (*S*)-Ph,Ph-ProNOP and (*S*)-Ph,Ph-oxo-ProNOP ligands (Scheme 4). These two earlier reported ligands provided lower turnover frequencies, i.e. 2.8 h^{-1} (*b*/*n* = 39/59, ee = 42%) and 5 h^{-1} (*b*/*n* = 29/68, ee = 40%), respectively. These results show clearly that, for platinum, the reaction rate increases with the lowering of the electron density on the phosphorous moieties

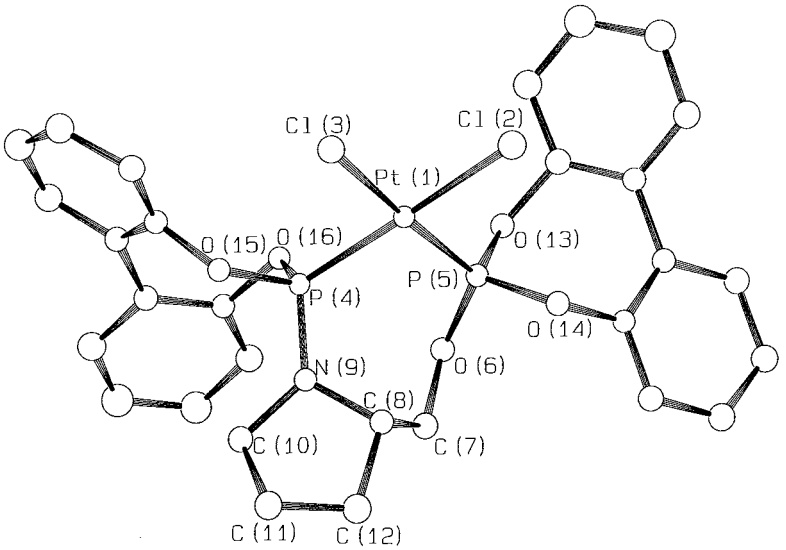

Fig. 1. Solid state structure and atom numbering of **5**. Hydrogen atoms are omitted for clarity.

of the ligand. Still, the branched to linear ratios were generally low with close to equal amounts of both regioisomers. Complex **6** provides a higher *b*/*n* ratio but with a nevertheless lower enantioselectivity into the branched aldehyde (15% ee) (run 8). As usually observed, ethylbenzene was formed along with the hydroformylation products during the course of the reaction. Unfortunately, for these two catalytic systems, this side-reaction is rather important with an average of 35% of ethylbenzene formed. The two solvents used, i.e. dichloromethane and toluene, did not have much effect on the properties of the catalyst (runs 1 and 2). Thus, because of the higher solubility of the starting complex in dichloromethane, the precatalyst was prepared in that solvent prior to the catalytic reaction. As presumed, lowering the partial pressure of hydrogen led to a smaller amount of hydrogenation (run 4). The highest asymmetric induction (44% ee) was found when the temperature was lowered to room temperature (run 7). This study proves that one chiral source is sufficient in the ligand to induce enantioselection but the latter is too low for an application. In addition to that single chirality, this family of ligands presents an intrinsic dissymmetry due to its chiral pool origin and the catalysis certainly benefits from that property.

On the other hand, for rhodium-based hydroformylations, compared to the previously reported ephedrine-based aminophosphonite–phosphite ligands [7e,10], modest regioselectivities in favour of the branched aldehyde and low enantioselectivities were obtained (runs 9–11). In addition, the reaction rates are significantly lower, too. Thus, not surprisingly, bisphenoxy moieties are not good substituents for phosphorous atoms in ligands designed for rhodium-catalysed enantioselective hydroformylations.

Table 3
Selected bond lengths (Å), bond angles (°), and deviations from the Pt(1)–Cl(2)–Cl(3)–P(4)–P(5) mean plane (Å)

Bond length			
Pt(1)–Cl(3)	2.331(3)	Pt(1)–Cl(2)	2.331(2)
Pt(1)–P(4)	2.202(2)	Pt(1)–P(5)	2.190(3)
P(4)–N(9)	1.620(7)	P(5)–O(6)	1.578(6)
P(4)–O(15)	1.595(6)	P(5)–O(13)	2.190(3)
P(4)–O(16)	1.600(6)	P(5)–O(14)	1.589(7)
N(9)–C(8)	1.492(9)	O(6)–C(7)	1.444(11)
N(9)–C(10)	1.485(11)	O(13)–C(29)	1.449(11)
O(15)–C(17)	1.412(9)	O(14)–C(40)	1.392(9)
O(16)–C(28)	1.413(C10)	C(22)–C(23)	1.472(12)
C(10)–C(11)	1.530(13)	C(34)–C(35)	1.472(12)
C(11)–C(12)	1.548(14)	C(7)–C(8)	1.521(14)
C(12)–C(8)	1.546(13)		
Bond angles			
Cl(2)–Pt–Cl(3)	87.07(10)	P(4)–Pt–P(5)	91.66(11)
Cl(2)–Pt–P(5)	89.76(11)	Cl(3)–Pt–P(4)	91.51(11)
Pt(1)–P(5)–O(6)	118.71(27)	Pt(1)–P(5)–O(14)	110.66(21)
Pt(1)–P(5)–O(13)	118.09(26)	O(6)–P(5)–O(14)	107.24(37)
O(6)–P(5)–O(13)	95.83(39)	O(14)–P(5)–O(13)	104.57(37)
Pt(1)–P(4)–N(9)	114.98(26)	Pt(1)–P(4)–O(15)	118.77(23)
Pt(1)–P(4)–O(16)	108.91(21)	N(9)–P(4)–O(15)	99.82(36)
N(9)–P(4)–O(16)	111.47(38)	O(15)–P(4)–O(16)	102.02(35)
P(4)–N(9)–C(8)	122.91(45)	P(4)–N(9)–C(10)	127.40(52)
C(10)–N(9)–C(8)	109.67(65)	P(4)–O(15)–C(17)	127.9(52)
P(4)–O(16)–C(28)	116.66(46)	P(5)–O(6)–C(7)	124.43(50)
P(5)–O(14)–C(40)	123.65(45)	P(5)–O(13)–C(29)	118.10(49)
Deviations from the mean plane			
Pt(1)	0.007(0)	N(9)	1.286(6)
Cl(2)	0.010(2)	O(13)	−1.377(6)
Cl(3)	0.013(2)	O(14)	1.037(5)
P(4)	0.009(2)	O(15)	0.050(5)
P(5)	−0.013(2)	O(16)	−1.368(5)
O(6)	0.234(6)		

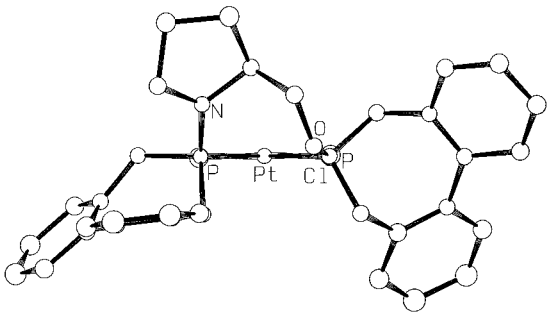

Fig. 2. View of the structure of **5** presenting the seven-membered metallacycle in a Newman-type projection.

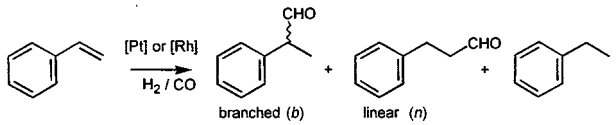

Scheme 3.

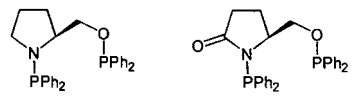

Scheme 4.

3. Conclusions

The syntheses of aminophosphonite–phosphite ligands and of the corresponding platinum complexes are readily carried out. The platinum complexes are stable under normal conditions and catalyse the asymmetric hydroformylation of styrene. These new catalysts are significantly more active than the previously reported Pt–AMPP. Nevertheless, only modest enantioselectivities are obtained and the hydrogenation side-reaction is observed in quite large amounts. The corresponding rhodium complexes present significantly poorer catalytic properties in styrene hydroformylation.

4. Experimental

4.1. General procedures

All reactions and manipulations were carried out under an atmosphere of dry N_2 using standard Schlenk-type glassware. Toluene and THF were distilled from benzophenone ketyl. Dichloromethane was distilled from calcium hydride. All solvents were freeze–thaw-degassed (three times) prior to use. The starting compounds $Pt(COD)Cl_2$ [18] and BPPCl [9] were synthesised according to the literature procedures. Styrene was filtered through alumina and freshly distilled just before use.

Elemental analyses were carried out by Laboratoires Wolff, Clichy, France. NMR spectra were obtained at room temperature in CD_2Cl_2 on a Bruker AC300 spec-

Table 4
Enantioselective hydroformylation of styrene involving Pt (**5** and **6**) [a] and rhodium (**Rh-3** and **Rh-4**) [b] precatalysts

Run	Complex	Solvent	Temperature (°C) (P_{CO}/P_{H_2} (atm))	Conversion (%) [c]	TOF (h^{-1}) [d]	Aldehydes (mol %) [e]	Select. b/n [e]	PhEt (mol. %) [f]	ee [g]
1	**5**	$PhCH_3$	50 (45/90)	97	38	70	53/47	30	26
2	**5**	CH_2Cl_2	50 (45/90)	98	35	65	55/45	35	30
3	**5**	$CH_2Cl_2/PhCH_3$ [h]	50 (45/90)	97	36	66	55/45	34	30
4	**5**	$CH_2Cl_2/PhCH_3$ [h]	50 (60/60)	98	38	80	53/47	20	30
5	**5**	$CH_2Cl_2/PhCH_3$ [h]	50 (45/90)	98	55	65	53/47	35	30
6	**5**	$CH_2Cl_2/PhCH_3$ [h]	30 (45/90)	54	20	66	53/47	34	38
7	**5**	$CH_2Cl_2/PhCH_3$ [h]	20 (45/90)	41	15	66	53/47	34	44
8	**6**	$CH_2Cl_2/PhCH_3$ [h]	20 (45/90)	30	15	65	66/34	35	15
9	**Rh-3**	toluene	80 (6/6)	100	15	100	63/37	0	5
10	**Rh-3**	toluene	40 (6/6)	15	1.3	100	88/12	0	19
11	**Rh-4**	toluene	40 (6/6)	20	1.7	100	72/28	0	15

[a] Conditions : platinum complex/$SnCl_2$ 1/1, substrate/catalyst = 1000, 18 h, 30 ml of solvent.

[b] Rhodium based hydroformylations were carried out in a stainless steel autoclave in toluene (30 ml) [Rh] = $5.41 \times 10-3$ mol L^{-1}; precatalyst **Rh-3**: in situ mixing of $Rh_4(CO)_{12}$ and **3**, **Rh-4**: in situ mixing of $Rh_4(CO)_{12}$ and **4**, ligand/Rh = 1.5; S/Rh = 400; t = 48 h.

[c] Styrene conversion.

[d] Turn over frequency: moles of aldehydes ($b+n$) formed per mole of platinum per hour.

[e] Selectivity into 2-(b) and 3-phenylpropanol (n) determined by GLC analysis.

[f] Selectivity into ethylbenzene determined by GLC analysis.

[g] See Section 4, all configurations are (S).

[h] Mixture of $CH_2Cl_2/PhCH_3$ 2/28 ml.

trometer operating at 300.1, 121.5 and 75 MHz for ^1H, $^{31}P\{^1H\}$, and $^{13}C\{^1H\}$, respectively. Proton and carbon chemical shifts were referenced to the deuterated solvent employed relative to tetramethylsilane (δ 0 ppm). Phosphorous chemical shifts are reported with positive values downfield from external 85% H_3PO_4 in D_2O (δ 0 ppm). The compositions of the catalytic reaction mixtures were determined by GLC analysis with a Delsi 30 gas chromatograph equipped with a flame ionisation detector using a 25 m × 0.25 mm CPSil 5-CB fused silica capillary column. The determination of the enantiomeric excesses was performed on a 25 m × 0.32 mm Chirasil-Dex column on the alcohols obtained after reduction of the aldehydes.

4.1.1. Synthesis of [(S)-N-(2,2'biphenoxyphosphino)-2-(2,2'biphenoxyphosphinoxymethyl) pyrrolidine (3)

Under nitrogen, a 100-ml Schlenk flask was charged with a magnetic stir bar, (*S*)-2-hydroxymethyl proline (**1**) (0.52 g, 5.16 mmol), THF (25 ml), and NEt_3 (5 ml). Then BPPCl (3.1 g, 12.38 mmol, 2.4 equivalents) in solution in THF (15 ml) was slowly added via cannula with stirring. A white precipitate formed instantaneously. The mixture was stirred vigorously and heated at 60°C overnight. The end of the reaction was checked by ^{31}P-NMR on an aliquot taken from the reaction medium. After cooling, the resulting crude reaction mixture was filtered under nitrogen through a pad of basic alumina (1 × 3 cm) and washed with Et_2O (2 × 20 ml). The solvents were evaporated from the combined filtrates under reduced pressure. The residue was further dried under oil pump vacuum, affording **3** as a white solid in 88% yield (2.4 g, 4.5 mmol). Anal. Found: C, 65.52; H, 4.90; N, 2.72. Calc. for $C_{29}H_{25}NO_5P_2$: C, 65.79; H, 4.75; N, 2.65%. ^1H-NMR (δ ppm): 1.60 (m, 2H), 1.71 (m, 1H), 1.81 (m, 1H), 2.69 (m, 1H), 3.11 (m, 1H), 3.67 (m, 1H), 3.85 (m, 2H), 6.95–7.39 (m, 16H). $^{13}C\{^1H\}$-NMR (δ ppm): 24.9 (s), 28.4 (d, $J_{CP} = 3.7$ Hz), 45.1 (s), 58.4 (dd, $J_{CP} = 25$ and 3 Hz), 67.3 (s), 122.0 (s), 122.2 (s), 124.8 (d, $J_{CP} = 8.2$ Hz), 125.4 (s), 129.4 (s), 129.6 (d, $J_{CP} = 4.3$ Hz), 129.9 (d, $J_{CP} = 14.6$ Hz), 130.2 (s), 150.0 (d, $J_{CP} = 5.2$ Hz), 150.2 (d, $J_{CP} = 5.8$ Hz), 151.8 (d, $J_{CP} = 5.3$ Hz), 152.1 (d, $J_{CP} = 5.2$ Hz). $^{31}P\{^1H\}$-NMR (δ ppm): 138.7 (s), 150.0 (s).

4.1.2. Synthesis of [(S)-N-(2,2'biphenoxyphosphino)-2-(2,2'biphenoxyphosphinoxymethyl) pyrrolidinone (4)

This compound was synthesised in the same way as **3**. The final filtration was carried out through a small pad of alumina (1 × 0.5 cm). Yield 86%. ^1H-NMR (δ ppm): 1.77 (m, 2H), 2.17 (m, 2H), 3.77 (m, 2H), 3.8 (m, 2H), 6.9–7.5 (m, 16H). $^{13}C\{^1H\}$-NMR (δ ppm): 24.3 (s), 31.2 (s), 46.3 (s), 57.4 (dd, $J_{CP} = 4.3$ and 7.9 Hz), 67.8 (d, $J_{CP} = 3.7$ Hz), 122.1 (s), 122.4 (s), 125.5 (d, $J_{CP} = 6.6$ Hz), 125.9 (s), 129.1 (s), 129.7 (d, $J_{CP} = 5.2$ Hz), 130.3 (d, $J_{CP} = 14.7$ Hz), 130.9 (s), 148.0 (d, $J_{CP} = 4.3$ Hz), 149.7 (d, $J_{CP} = 5.2$ Hz), 149.8 (d, $J_{CP} = 4.7$ Hz), 150.4 (d, $J_{CP} = 3.2$ Hz), 182.6 (d, $J_{CP} = 15.9$ Hz). $^{31}P\{^1H\}$-NMR (δ ppm): 137 (s), 145 (s).

4.1.3. [(S)-N-(2,2'biphenoxyphosphino)-2,2'biphenoxyphosphinoxymethyl)pyrrolidine] dichloroplatinum(II) (5)

A Schlenk tube was charged with $Pt(COD)Cl_2$ (0.1 g, 0.27 mmol), CH_2Cl2 (10 ml) and a stir bar. A solution of **3** (0.155 g, 0.29 mmol, 1.1 equivalents) in CH_2Cl_2 (5 ml) was added via cannula with stirring. After 30 min vigorous stirring at room temperature (r.t.), the solvent was evaporated from the colourless solution under vacuum. Then, the white residue was washed with diethyl ether (2 × 10 ml) and finally dried under vacuum providing compound **5** in 97% yield (0.202 g, 0.25 mmol). Anal. Found: C, 42.31; H, 3.38; N, 1.60; O, 9.60. Calc. for $C_{29}H_{25}Cl_2NO_5P_2Pt{\cdot}0.5CH_2Cl_2$: C, 42.29; H, 3.12; N, 1.67; O, 9.55%. ^1H-NMR (δ ppm): 1.73 (m, 1H), 1.80 (m, 1H), 2.12 (m, 2H), 2.69 (m, 2H), 3.3 (m, 1H), 3.9 (m, 1H), 4.6 (m, 1H). $^{31}P\{^1H\}$-NMR (δ ppm): 72 (d, $J_{PP} = 28$, $J_{Pt-P} = 5792$ Hz, satellites), 85 (d, $J_{PP} = 28$, $J_{Pt-P} = 5392$ Hz, satellites).

4.1.4. [(S)-N-(2,2'biphenoxyphosphino)-2,2'biphenoxyphosphinoxymethyl)pyrrolidinone] dichloroplatinum(II) (6)

This compound was synthesised in the same way as **5**. Yield 98%. $^{31}P\{^1H\}$-NMR (δ ppm): 86 (d, $J_{PP} = 4.2$, $J_{Pt-P} = 5833$ Hz, satellites), 90 (d, $J_{PP} = 4.2$, $J_{Pt-P} = 5658$ Hz, satellites).

4.1.5. Crystal structure of 5·CH_2Cl_2

Suitable crystals were obtained as colourless prisms by slow crystallisation from dichloromethane. The crystal selected was mounted for data collection on an Enraf–Nonius CAD-4 diffractometer, as summarised in Table 1. The intensities of three representative reflections, which were measured after every 2 h, remained constant throughout data collection, indicating crystal and electronic stability. Data were corrected for Lorentz and polarisation effects but not (since the faces were not identified easily) for absorption. The atomic coordinates of the platinum atom were deduced from the Patterson function, and the positions of chlorine, phosphorous, oxygen, nitrogen, and carbon atoms were identified from successive difference-Fourier syntheses. All positional and thermal parameters were refined with SHELX-76 [19]. The atomic scattering factors for neutral atoms, as well as the anomalous dispersion correction coefficients, were taken from Ref. [20]. The presence of a solvent molecule highly disordered in the structure did not permit us to localise the hydrogen atoms. Refinement of all atoms yielded a final $R = 0.039$ and $R_w = 0.045$, with $w = 1/[\sigma^2(F) + 0.00369F^2]$ in the final stages.

4.1.6. Catalytic asymmetric platinum-based hydroformylations

All catalytic reactions were conducted in a magnetically stirred and double-walled 60-ml stainless steel reactor. In a typical experiment, a solution of the cocatalyst $SnCl_2 \cdot 2H_2O$ (0.1 mmol) and of the platinum complex (0.1 mmol) in CH_2Cl_2 (2 ml) was introduced in the reactor under dinitrogen. Then, styrene (100 mmol) and the internal standard (*n*-decane) in toluene (28 ml) were introduced. The reactor was sealed, pressurised to 130 atm with $CO–H_2$ (1/2) and heated at 50°C. The reaction was monitored by GLC analysis of aliquots of the reaction mixture. When the reaction was stopped, the reactor was cooled to r.t. and depressurised. The pale-yellow solution was analysed by GLC to determine the selectivities into hydroformylated (branched and normal) products and ethylbenzene. Pentane was then added to the crude reaction mixture to precipitate the catalyst. The resulting solid was filtered off and the remaining solution was concentrated by rotatory evaporation. The crude mixture was then dissolved in diethylether (20 ml) and an excess of $LiAlH_4$ was added. After 1 h stirring at r.t., the medium was cautiously quenched with aqueous HCl (1 N) (10 ml). The aqueous layer was extracted two times with diethylether (10 ml). The combined organic phases were washed with water (2×20 ml), dried over $MgSO_4$, concentrated by rotatory evaporation, and analysed by chiral GC.

4.1.7. Catalytic asymmetric rhodium-based hydroformylations

In a typical experiment, a Schlenk tube was charged with a stir bar, the ligand (0.216 mmol), $Rh_4(CO)_{12}$ (26.9 mg, 0.036 mmol), and toluene (10 ml). After 15 min stirring at r.t., the solution was transferred via cannula to a 60-ml stainless steel double-walled autoclave equipped with a stir bar. After a N_2 purge, styrene (6 g, 57.6 mmol), diluted in toluene (10 ml) (substrate = 2.16 mol l^{-1}), was also added via cannula. The autoclave was pressurised to 12 bar of syn-gas ($H_2–CO$ 1/1) and then heated to the desired temperature. The pressure was kept constant throughout the whole reaction by using a gas reservoir along with a pressure regulator. The workup and determination of conversion, chemo-, regio-, and enantioselectivities were carried out as reported above for platinum-based catalytic runs.

5. Supplementary material

Crystallographic data for the structural analysis have been deposited with the Cambridge Crystallographic Data Centre, CCDC No. 154572 for $PtCl_2\{(S)$-BPProNOP$\}$. Copies of this information may be obtained free of charge from The Director, CCDC, 12 Union Road, Cambridge CB12 1EZ, UK (Fax: +44-1223-336033; e-mail: deposit@ccdc.cam.ac.uk or www: http://www.ccdc.cam.ac.uk).

Acknowledgements

This work has been supported financially by the Centre National de la Recherche Scientifique and the Ministère de l'Enseignement Supérieur. We thank Olivier Lot and Dr Hervé Bricout for initial experiments, and Catherine Méliet for skilful NMR assistance.

References

[1] C. Botteghi, S. Paganelli, A. Schionato, M. Marchetti, Chirality 3 (1991) 355.
[2] (a) J.P. Rieu, G. Boucherle, H. Cousse, G. Mouzin, Tetrahedron 42 (1986) 4095. (b) H.R. Sonawane, N.S. Bellur, J.R. Ahuja, D.G. Kulkarni, Tetrahedron: Asymmetry 3 (1992) 163.
[3] Review articles on asymmetric hydroformylation: (a) S. Gladiali, J. Bayon, C. Claver, Tetrahedron: Asymmetry 7 (1995) 1453. (b) F. Agbossou, J.-F. Carpentier, A. Mortreux, Chem. Rev. 95 (1995) 2485. (c) G. Consiglio, in: I. Ojima (Ed.), Catalytic Asymmetric Syntheses, VCH, Weinheim, 1993, p. 273. (d) M. Beller, B. Cornils, C.D. Frohning, V.W. Kohlpainter, J. Mol. Catal. 104 (1995) 17. (e) K. Nozaki, H. Takaya, T. Hiyama, Top. Catal. 4 (1997) 175.
[4] (a) N. Sakai, S. Mano, K. Nozaki, H. Takaya, J. Am. Chem. Soc. 115 (1993) 7033. (b) N. Sakai, K. Nozaki, H. Takaya, J. Chem. Soc. Chem. Commun. (1994) 395. (c) T. Horiuchi, T. Ohta, K. Nozaki, H.Takaya, J. Chem. Soc. Chem. Commun. (1996) 155.
[5] (a) N. Sakai, K. Nozaki, K. Mashima, I. Takaya, Tetrahedron: Asymmetry 3 (1992) 583. (b) J.E. Babbin, G.T. Whiteker, WOUS patent 911 518, 1992 (to Union Carbide Corp.), Chem. Abstr. 119 (1993) 159872h. (c) G.J.H. Buisman, P.C.J. Kramer, P.W.N.M. van Leeuwen, Tetrahedron: Asymmetry 4 (1993) 1625. (d) G.J.H. Buisman, M.E. Martin, E.J. Vos, A. Klootwijk, P.C.J. Kramer, P.W.N.M. van Leeuwen, Tetrahedron: Asymmetry 7 (1995) 719.
[6] (a) G. Consiglio, S.C.A. Nefkens, A. Borner, Organometallics 10 (1991) 2046. (b) L. Kolar, P. Sandor, G. Szalontai, J. Mol. Catal. 67 (1991) 191. (c) A. Scrivanti, S. Zeggio, V. Boeghetto, U. Matteoli, J. Mol. Catal. 101 (1995) 217. (d) J.K. Stille, H. Su, P. Brechor, G. Parrinello, L.S. Hegedus, Organometallics 10 (1991) 1183. (e) S. Cserépi-Szücs, J. Bakos, Chem. Commun. (1997) 635.
[7] (a) S. Mutez, A. Mortreux, F. Petit, Tetrahedron Lett. 29 (1988) 1911. (b) Y. Pottier, A. Mortreux, F. Petit, J. Organomet. Chem. 370 (1989) 333. (c) S. Naili, J.-F. Carpentier, F. Agbossou, A. Mortreux, G. Nowogrocki, J.-P. Wignacourt, Organometallics 14 (1995) 401. (d) A.M. Bandini, G. Banditelli, E. Cesarotti, G. Minghetti, B. Bovio, Inorg. Chem. 31 (1992) 391. (e) R. Ewalds, E.B. Eggeling, A.C. Hewat, P.C.J. Kramer, P.W.N.M. van Leeuwen, D. Vogt, Chem. Eur. J. 6 (2000) 1496.
[8] (a) A. Roucoux, L. Thieffry, J.-F. Carpentier, M. Devocelle, C. Méliet, F. Agbossou, A. Mortreux, Organometallics 15 (1996) 2440. (b) F. Agbossou, J.-F. Carpentier, C. Hatat, N. Kokel, A. Mortreux, Organometallics 14 (1995) 2480.

[9] G.J.H. Buisman, P.C.J. Kramer, P.W.N.M. van Leeuwen, Tetrahedron: Asymmetry 4 (1993) 1625.
[10] O. Lot, I. Suisse, A. Mortreux, F. Agbossou, J. Mol. Catal. 164 (2000) 125.
[11] P.S. Pregosin, R.W. Kunz, in: P. Diehl, E. Fluck, R. Kosfeld (Eds.), NMR 16 Basic Principles and Progress: ^{31}P and ^{13}C NMR of Transition Metal Phosphine Complexes, Springer, Berlin, 1979.
[12] (a) T.T. Derencsényi, Inorg. Chem. 20 (1981) 665. (b) G.G. Mather, A. Pidcock, G.J.N. Rapsey, J. Chem. Soc. Dalton Trans. (1973) 2095. (c) L.M. Green, Y. Park, D.W. Meek, Inorg. Chem. 27 (1988) 1658. (d) J.A. Rahn, L. Baltusis, J.H. Nelson, Inorg. Chem. 29 (1990) 750. (e) A.W. Verstuyft, D.A. Redfield, L.W. Cary, J.H. Nelson, Inorg. Chem. 15 (1976) 1128.
[13] E. Cesarotti, M. Grassi, L. Prati, J. Chem. Soc. Dalton Trans. 1 (1989) 161.
[14] F. Hapiot, F. Agbossou, C. Méliet, A. Mortreux, G.M. Rosair, A.J. Welch, New J. Chem. 21 (1997) 1161.
[15] S. Cserépi-Szücs, G. Huttner, L. Zsolnai, J. Bakos, J. Organomet. Chem. 586 (1999) 70.
[16] Square planar complexes bearing AMPP ligands — Platinum: (a) S. Naili, J.-F. Carpentier, F. Agbossou, A. Mortreux, New J. Chem. 21 (1997) 919. (b) Ref. [7c]. Rhodium: (d) V.A. Pavlov, E.I. Klabunovsky, Y.T. Struchkov, A.A. Voloboev, A.I. Yanovsky, J. Mol. Catal. 14 (1988) 119. (e) E. Cesarotti, A. Chiesa, G. Ciani, A. Sironi, J. Organomet. Chem. 251 (1983) 79. Palladium: (f) E. Cesarotti, M. Grassi, L. Prati, F. Demartin, J. Organomet. Chem. 370 (1989) 407.
[17] Ruthenium complexes bearing AMPP ligands: (a) E. Cesarotti, L. Prati, A. Sironi, G. Ciani, C. White, J. Chem. Soc. Dalton Trans. 5 (1987) 1149. (b) Ref. [14].
[18] D. Drew, J.R. Doyle, A.G. Shaver, Inorg. Synth. 13 (1972) 47.
[19] G. Sheldrick, SHELX-76, System of Crystallographic Computer Programs, University of Cambridge, Cambridge, UK, 1976.
[20] D.T. Cromer, International Tables for X-ray Crystallography, vol. IV, Kynoch Press, Birmingham, UK, 1974.